Article

A General Signal Amplification Strategy for Non-Faradaic Impedimetric Sensing: Trastuzumab Detection employing a Peptide Immunosensor

Juan Liu, Mohammad Muhsin Chisti, and Xiangqun Zeng

Anal. Chem., **Just Accepted Manuscript** • DOI: 10.1021/acs.analchem.6b04570 • Publication Date (Web): 03 Mar 2017

A General Signal Amplification Strategy for Non-Faradaic Impedimetric Sensing: Trastuzumab Detection employing a Peptide Immunosensor

Juan Liu[1], Mohammad Muhsin Chisti[2], Xiangqun Zeng[1]*

[1]Department of Chemistry, Oakland University, Rochester, MI 48309

[2] Karmanos Cancer Institute, Detroit, MI 48201

ABSTRACT: A label free and reagent free peptide mimotope capacitive biosensor is developed for cancer drug (Trastuzumab) quantification based on non-Faradaic readout. The low sensitivity issue of capacitive biosensor was overcomed with two innovations: peptide mimotope mixed SAM biointerface and dilution of the analysis buffer. Signal amplification was achieved through dilution of the PBS buffer to tune C_{dl} to dominate the overall capacitance change upon target binding, which contribution is often negligible without dilution. After 1000 times dilution, limit of detection is lowered 500 times (0.22 μg/mL) and the sensitivity increased 20 times (0.04192 (μg/mL)$^{-1}$) than in undiluted PBS. The proposed signal amplification strategy is more straightforward and practical compared to biorecognition element engineering and other strategies. The proposed method has further applied to planar electrode for optimizing sensing response time in less than 1 minute.

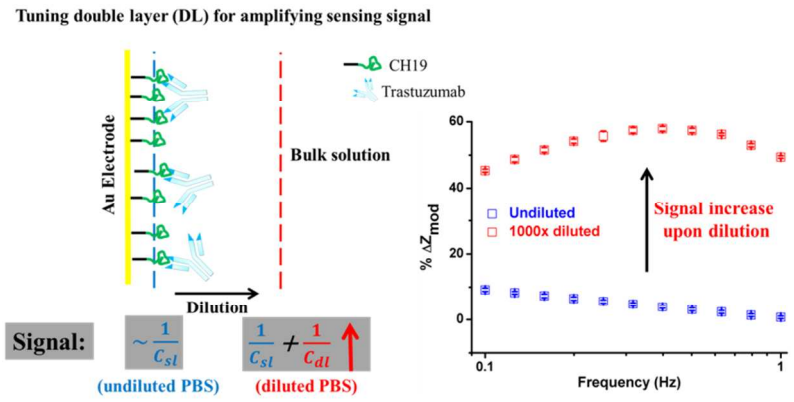

Introduction

In recent decades, biosensor technology has advanced significantly. However, few of the current reported biosensors can satisfy the requirements for translation to the point of care clinical applications in terms of accuracy, cost, portability, and accessibility. Electrochemical techniques are historically proven to be low cost, portable and easy-to-use making them ideal platforms for developing biosensors for the point of care applications. Among various electrochemical techniques, electrochemical impedance spectroscopy (EIS) is especially suitable for the biosensor applications. EIS uses an AC (alternating current) excitation potential, E_{ac}, of a very small amplitude, often in the range of 5 to 10 mV peak to peak AC voltage, the resulting AC current, i_{ac}, is measured so that the impedance of the electrochemical system can be obtained. Due to the small amplitude of the excitation waveforms, EIS measurements cause minimal perturbation of the electrochemical system, making it non-invasive for probing the binding reactions at the surface of the biosensor electrode.

There are two major types of EIS methods that are currently used in biosensor readouts: Faradaic impedance spectroscopy and non-Faradic impedance spectroscopy. Faradic impedance spectroscopy involves the use of redox probes such as $K_3Fe(CN)_6/K_4Fe(CN)_6$ to indirectly probe the bio-interaction occurring at the electrode interface. Thus, it requires the design and incorporation of redox probes in the detection system. This is not desirable for point of care applications since either an additional redox probe needs to be added or a solid redox probe needs to be designed and incorporated into the detection system. In contrast, non-Faradic impedance method is direct, simple and reagentless without the need of the use of any redox probe. In non-Faradic impedance methods, the binding of the target molecules with the immobilized biorecognition element, e.g., enzymes, antigens/antibodies or DNA on the electrodes or semiconductor surfaces alters the capacitance of the conductive or semiconductive electrodes allowing the measurements of the biorecognition events at the electrode surface directly.[1-6] Since no redox molecule is required, capacitive sensor based on the non-Faradic impedance method is reagentless, label free and thus non-invasive compared to Faradaic impedance where redox probes are utilized. Due to these merits, capacitive biosensor have been widely used for study of cell exocytosis,[7] interfacial effects of neuronal cell growth and differentiation,[8] and detection of biomarker,[9] protein (HSA),[2] antibody,[5] DNA[4,10] and ions.[6,11] However, non-faradic impedance methods are not very sensitive since the signal change at electrode surface is based on the change of differential capacitance properties before and after the binding reactions at the interface which is typically very small. The binding reactions between the probe molecules such as antibodies or DNAs with the targeted analyte normally result in a less than 10% change in the capacitance which is often too small to be distinguished from the non-specific interactions or molecule trapping at the electrode surface during the biological binding reactions.

In this work, we addressed the low sensitivity issue of the non-faradic impedance methods for biosensor applications with two innovative approaches. First, rather than using antibodies or proteins as recognition elements, pep-

tide mimotope self-assembled monolayer (SAM) was designed and used as the recognition element. Peptide mimotopes with small size (MW: 1-3KD) not only are significantly low cost but also allow a relatively dense and uniform SAM immobilization of recognition elements. Thus, peptide mimotope SAMs give less opportunity for non-specific interactions or molecule trapping at the electrode surface compared to their antibodies or protein counterparts. Peptide mimotope SAM biointerface is more homogeneous and closely resemble an ideal capacitor. This is beneficial to provide stable baseline for the impedance based readout methods. Second, the binding reactions are measured at a diluted PBS buffer with low ionic strength. Our results show that sensing signals can be amplified when measured at low ionic strength buffer solutions. As shown in scheme 1 and detailed results and discussion in the later section, through dilution, the baseline double layer capacitance is tuned to be small enough to also contribute and dominate the signal in addition to sensing layer capacitance, subsequently leading to a bigger change of the interface capacitance upon binding reactions. Both approaches increase the signal to noise ratio and the sensitivity of the biosensor based on the non-faradic impedance readout. To validate the above approach, we select a cysteine containing peptide mimotope CH19 (CGSGSGSQLGPYELWELSH) that mimics the Human Epidermal Growth Factor Receptor (HER2) antigen as the peptide for study. CH19 was demonstrated to bind specifically to Trastuzumab (also called Herceptin), a monoclonal antibody cancer drug.[12] A spacer peptide CGSGSGS (CS7) was used to further passivate the electrode surface to minimize non-specific adsorption. The "mixed" CH19/CS7 SAM allows the formation of a compact sensing layer. The binding of CH19 biointerface with Trastuzumab (Herceptin) was characterized at both PBS buffer (undiluted) and 1000 times diluted PBS buffer using non-faradic impedance method. Our results show a SAM of CH19 responses quantitatively to Trastuzumab concentrations via differential capacitance changes. Trastuzumab detection methods, mostly using enzyme-linked immunosorbent assay (ELISA),[13-15] are summarized in Table SI1. To the best knowledge of the authors, the sensing method described in this report is the first non-invasive electrochemical method for Trastuzumab detection. The simple and straightforward dilution method is shown to allow signal amplification by increasing the signal to noise ratio (reduce the baseline double layer capacitance as well as increase the change of the capacitance due to binding reaction). This work provides a general signal amplification strategy that resolves the small capacitance/signal change issue commonly encountered in non-faradic impedance based biosensors and could be a potentially powerful approach for label free, reagent free impedance sensor development.

Materials and Methods

1. Materials and chemicals:

Peptides, designated as CH19 (sequence: CGSGSGSQLGPYELWELSH, purity >95.84%, Mw 2007.14) and CS7 (sequence: CGSGSGS, purity 95.99%, Mw 553.54)), were chemically synthesized by Bio. Basic, Inc. (Ontario, Canada) and received in a lyophilized condition. The sequence and quality of both peptides was confirmed and assessed by matrix-assisted laser desorption/ionization (MALDI) mass spectrometry analysis, and the purity was determined by high performance liquid chromatography (HPLC). Therapeutic monoclonal antibodies (mAbs) such as Trastuzumab (Herceptin), Bevacizumab (Avastin), Ofatumumab (Arzerra), Obinutuzumab (Gazyva), Panitumumab (Vectibix), and Rituximab (Rituxan) were provided by Beaumont Hospital, Royal Oak, Michigan. Gold working electrode (2mm diameter) was purchased from CH Instruments, Inc. (Austin, TX). Gold wire (0.025mm diameter, annealed, 99.95%), silver conductive adhesive paste and E-120HP hysol epoxy adhesive were obtained from VWR (Radnor, PA). Corning 8161 patch clamp glass capillaries (LB16, 1.50 mm outer diameter, 1.10 mm inner diameter, wall thickness 0.20mm, length 100mm) and tungsten rods (0.010 × 3.000 in.) were acquired from Warner Instrument (Hamden, CT) and AM Systems, Inc. (Sequim, WA) respectively. Microcut/Carbimet discs (240 grit, 600 grit and 1200 grit), microcloth, 1.00 μm and 0.05 μm alumina micropolish powder for polishing electrodes were purchased from Buehler (Lake Bluff, IL). Phosphate Buffer Saline (PBS, 1X, pH 7.4) was purchased from Thermo Fisher Scientific (Waltham, MA). It has a composition of 155 mM NaCl, 1mM KH_2PO_4, and 3mM Na_2HPO_4-$7H_2O$. 10x, 100x, and 1000x diluted PBS were prepared by directly diluting the 1x PBS with deionized H_2O without adjusting pH.

2. EIS methods and protocols

Microelectrode Fabrication: 25 μm (diameter) gold electrode is fabricated following previous report[16-19]: Briefly, a 25 μm gold wire is connected to tungsten rod using silver conductive adhesive paste. The gold/tungsten assembly is inserted into glass capillary and then the gold wire is sealed into the glass capillary using a gas flame. The other end of glass capillary is sealed with Hysol epoxy adhesive to fix the gold/tungsten assembly inside the glass capillary. The glass capillary is polished on 240, 600 and 1200 grit sand papers sequentially to remove excess glass to expose the gold surface, resulting in a 25 μm gold electrode.

Cleaning: Before surface functionalization, 25 μm (2 mm) gold electrodes are cleaned by hand polishing with 1.00 and 0.05 μm alumina slurry on microcloth for 2 min, sequentially. After each polishing, electrodes are sonicated in ethanol and H_2O, respectively, each for 5 min to remove adsorbed alumina polishing powder. Then, the gold electrodes are further cleaned by cycling potential from -0.35V to 1.5V in 0.05M sulfuric acid until a reproducible cyclic voltammogram of gold oxidation is obtained.

Modification: A two-step surface modification procedure is used for the peptide biosensor fabrication. First,

the clean gold electrode is incubated into 1mM CH19 peptide (probe) solution overnight (~26h) at 4°C to form a self-assembled monolayer of CH19 peptide, followed by immersing the CH19 functionalized electrode into 1μg/μL CS7 overnight (~15h) at 4°C for further surface passivation.

Biointerface characterization: Cyclic voltammetry in 1 mM 1:1 $K_3Fe(CN)_6$: $K_4Fe(CN)_6$ before and after peptide surface modification is first used to characterize surface functionalization. Then single frequency Electrochemical Impedance Spectroscopy (single frequency EIS) is used for Trastuzumab titration. The impedance of fabricated sensor in PBS (both diluted and undiluted) is monitored for Trastuzumab quantification. A three-electrode system is used in all electrochemical experiments, which utilizes either 25μm or 2mm gold electrode as working electrode (WE), platinum wire as counter electrode (CE) and home-made Ag/AgCl wire as quasi-reference electrode (QRE). Before impedance monitoring, the biosensor is preconditioned at 0V (the same as the frequency monitored using single frequency EIS technique) for 1200s to facilitate the constant electrode/solution interface formation so that a stable impedance baseline can be established. When a stable impedance background is achieved, varying amount of Trastuzumab was added into the biosensor cell. The impedance is monitored at 0V DC (direct current) (vs. Ag/AgCl QRE) and 5mV AC at 0.2 Hz frequency (this is an optimized condition based on 2mm sensor data). Note, preconditioning experiment is a critical step to ensure a constant baseline for this methodology since it allows the peptide SAM to establish an equilibrium state for detection. All experiments are carried out using Gamry Multichannel Potentiostat (Gamry Instruments).

3. Quartz Crystal Microbalance (QCM) methods and protocols

The peptide biointerface is also fabricated on an AT cut quartz wafer coated with 1000-Å of gold of ~0.23 cm^2 geometric area (International Crystal Co.). The immobilized CH19 peptide mimotope density is characterized by monitoring the oscillating frequency before and after CH19 peptide immobilization.

Electrode Cleaning: Before surface functionalization, the gold coated quartz wafer electrode is cleaned with 1:1 (v/v) mixture of concentrated nitric acid and sulfuric acid, rinsed with copious amounts of ethanol and water in series, then dried in nitrogen. This cleaning is repeated for three times.

Peptide biointerface fabrication: The cleaned gold coated quartz wafer electrode is mounted into a home-made Kel-F cell sealed by two viton O-rings. The same two-step surface modification procedure is used for immobilization of the CH19/CS7 mixed peptide SAM as discussed above. After surface functionalization, the immobilized gold QCM electrode is washed with PBS three times to remove non-specific adsorbed peptides.

Biointerface characterization: The peptide biointerface modified electrode mounted in the home-made Kel-F sensor cell is filled with 1.2mL PBS and placed into a Faraday cage to reduce noise from environment. The PBS solution is continuously stirred during QCM measurement. Network/Spectrum/Impedance Analyzer (Agilent 4395A) is used for monitoring the frequency change and the damping resistance change caused by the analyte (Trastuzumab) addition. The frequency change before and after surface functionalization is used to characterize the immobilized peptide density.

RESULTS AND DISCUSSION

1. Impedance Sensing Model of a Peptide SAM Biointerface

The non-Faradic impedance method is based on the change of the electrical double layer properties for sensing the interface binding reactions. The electric double layer refers to two parallel layers of charge at the electrode/solution interface. The first layer, the surface charge (either positive or negative), comprises ions adsorbed onto the electrode due to electrostatic and/or chemisorptions. The second layer is composed of counter ions attracted to the surface charge via the coulomb force, electrically screening the first layer. The electric double layer exists in almost all interfaces. As shown in Scheme 1b, Helmholtz developed an electrical double layer model. When a metallic electrode in contact with a solution is polarized by an applied potential, the induced charge restricted on electrode surface will attract counter ions in solution due to electrostatic interaction for the charge compensation and this double layer is equivalent to an electrical capacitor in which there are two layers of charges separated by a fixed distance at the electrode/electrolyte interface.[20] The potential drop between these two charged layers is linear and the double layer capacitance is a constant. This is an oversimplification as differential capacitance is potential and solution dependent.[21] Later Gouy-Chapman proposed a model which includes a diffuse layer of charge in solution phase.[22-24] The Gouy-Chapman model predicted a V-shape differential capacitance, which is an improvement over Helmhotz model but the predicted differential capacitance is much larger than the actual capacitance.[25] The abnormally higher capacitance predicted results from the assumption that ions are considered to be point charge thus it can approach electrode infinitely close, which is not realistic as ions have their own finite sizes. Meanwhile in consideration of a high compact layer at high polarization or in concentrated solution, Stern combined Helmholtz and Gouy-Chapman model.[26] The proposed Gouy-Chapman-Stern model consists of compact Helmholtz layer in series with an extended diffuse layer. In 1947, Grahame further modified Stern's model and introduced the three-layer model by proposing that solvent molecule and other species can be specifically adsorbed onto the electrode surface.[21] The closest layer to the electrode surface is the specifically adsorbed layer called inner Helmholtz plane (IHP). Followed by the outer Helmholtz plane (OHP) formed by nonspecifically attracted compact solvated counter ions through electrostatic interaction. The loosely

attracted solvated counter ions form the diffusion layer. This three-layer model currently is the well-accepted model for the electric double layer. As shown in Scheme 1b, two capacitances can be associated with the electrical double layer. The first, C_{OHP}, is the differential capacitance of the OHP and the second, $C_{Diffuse}$, corresponds to that of the diffused region. The overall capacitance is then simply given by the sum of the two (equation 1):

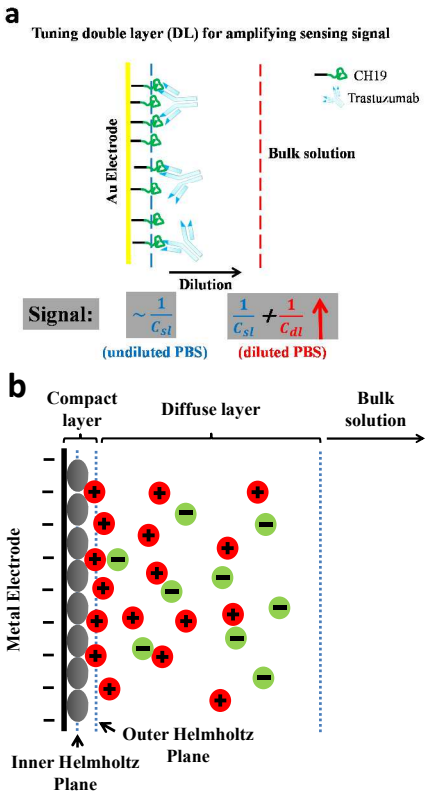

Scheme 1. Scheme (a) and model (b) for the peptide mixed SAM biointerface on gold electrode.

$$\frac{1}{C} = \frac{1}{C_{OHP}} + \frac{1}{C_{Diffuse}} \quad (1)$$

$$C = \frac{\varepsilon A}{\delta} \quad (2)$$

$$\frac{1}{C} = \frac{1}{C_{dl}} + \frac{1}{C_{sl}} \quad (3)$$

where C (capitalized) is capacitance, A is area, ε is permittivity and δ is distance.

Since the total capacitance depends on the reciprocals of the two separated contributions, it is the smallest capacitance that dominates the capacitance. When there is no specific adsorption, then C_{OHP} is independent of the electrolyte concentration as only solvent molecules are present within this layer. In contrast, $C_{Diffuse}$ is very sensitive to the ion excesses or depletions within the diffuse layer. Shown in Fig.2b, when electrode is modified with adsorbed SAM of peptide, the electrode-electrolyte interface is very different from the traditional electrical double layer. It is typically modeled with C_{Au}, an unmodified electrode (e.g., for a polycrystalline Au electrode, C_{Au} is about 40-60 μF/cm² depending on the applied potential), double layer capacitance (C_{dl}) and a variable capacitance (C_{sl}) depending on the electrode surface modifier (sensing layer), results from voltage drop across the sensing layer. They are connected as series elements. Assuming C_{Au} is a constant at a fixed potential, the capacitance equation can be expressed as C_{dl} and C_{sl} in equation 3. The surface modification results in a decrease of the differential capacitance due to two factors: 1) the thickness of the double layer increases due to the introduction of sensing layer to the electrode surface; 2) The change of dielectric properties of the interface. Water is replaced by an organic SAM layer with a lower dielectric constant. The differential capacitance of functionalized electrode can be represented by equation 3, which consists of C_{dl} and C_{sl}.[27-29]

The C_{dl} has a typical value in the range of 10~40 μF/cm²,[21,25] while organic molecule (peptide, alkanethiol, antibody) formed SAM with a smaller C_{sl} <10 μF/cm².[5,30-32] For example, helical peptides and amyloid peptides with a capacitance < 4 μF/cm² are reported.[32] Alkanethiol SAM (~2 nm length) has a capacitance of 1-2 μF/cm².[5] Antibody linked to self-assembled thioctic acid has an even smaller capacitance < 1 μF/cm².[31] Based on equation 3, differential capacitance is dominated by smaller one of C_{sl} and C_{dl}. Thus C_{sl}, which is always smaller than C_{dl} will dominate.[28] In other words, the capacitance change of the sensing layer C_{sl} upon target binding is the main sensing signal for non-faradaic impedimetric sensing.[33] The smaller C_{sl}, the relative larger C_{sl} change, thus larger signal can be obtained. Our data showed that upon the CH19 peptide and Trastuzumab binding, the impedance/capacitance increased ~9% in undiluted 1x PBS which is comparable to others' non-Faradaic sensing reports.[4,5] Our data also showed that C (mainly C_{sl}) change is quite small upon target binding/hybridization reactions indicating contribution from C_{sl} (C_{sl} change) is intrinsically small. For example, ~5% change of the impedance was observed upon anti-FMDV (foot-and-mouth-disease-virus)-ab binding to surface immobilized FMDV epitope by Rickert et. al.[5] Ma et. al. also reported a 10% impedance increase after DNA hybridization.[4] This small signal change is a common issue for capacitive based biosensor. In order to increase the electrochemical impedance signal, fluorescence labeling method was used in which the signal is amplified by using alkaline phosphatase enzyme (immobilized on the electrode surface through streptavidin-biotin interaction) to catalyze conversion of soluble ELF 97 (a fluorophore) into insoluble product that precipitates onto electrode surface. But unsatisfactory results were obtained using this strategy. Signal amplification using Horse Radish Peroxidase induced precipitation[3] and gold nanoparticles induced silver precipitation for signal enhancement based on interdigitated Al/Al_2O_3 microelectrode[34] were also reported. All these amplification methods are not simple and require additional steps. The biosensors using these methods are also not reusable, thus they are not suitable for real-time sensing.

Since the smaller C_{sl}, the larger signal, most current approaches for impedance based sensing focus on the modification of the sensing layer to achieve signal ampli-

fication. However, it is time-consuming and expensive. In this work, we design a fundamentally straightforward amplification strategy to achieve signal amplification by tuning the C_{dl} through solution buffer dilution to allow C_{dl} to contribute and even dominate the capacitance sensing signal. As the solution buffer is diluted, the solution ionic strength decreases which results in a decrease of the double layer capacitance C_{dl} due to the increase of the thickness of the diffuse layer, which in turn decreases the total differential capacitance.[25] By this way, C_{dl} competes with C_{sl} to contribute even could dominate the sensing signal (impedance). We measure the CH19/CS7 peptide SAM thickness at diluted and undiluted buffer conditions using ellipsometry and results show the peptide thickness in both conditions are similar suggesting that the dilution effect on C_{sl} is negligible.[35] Our method achieves signal amplification by optimizing the differential capacitance (impedance) through tweaking the baseline of the double layer capacitance so that any changes due to the binding reactions can be measured more sensitively. It is well known, C_{dl} depends on the concentration of the electrolyte and potential.[21] C_{dl} decreases as the ion concentration decreases which results in an expanded double layer (diffuse layer).[21,25] Therefore, simply by diluting the solution, C_{dl} can be tuned to be small enough, thus C_{dl} change is significant to contribute to differential capacitance change. Furthermore, the total impedance is monitored and used instead of the capacitance, as it is directly measured in the non-Faradaic impedance experiment.

2. Characterization of the CH19/CS7 peptide SAM and its binding with Trastuzumab

Cyclic Voltametry (CV) and Quartz Crystal Microbalance (QCM) are used to characterize the peptide biointerface fabrication. QCM was used to determine CH19 probe density on the surface by measuring the frequency change before and after CH19/CS7 peptide immobilization. Based on Sauerbrey equation, the peptide probe density is determined to be ~$6x10^{14}$ molecules/cm^2. CV is used to further verify the success of the immobilization of the "mixed" SAM of CH19/CS7 using an added redox probe $K_3Fe(CN)_6/K_4Fe(CN)_6$. The accessibility of redox probes to the peptide modified electrode surface is hampered with decreases of the current peaks of $K_3Fe(CN)_6/K_4Fe(CN)_6$ (Figure S1). As shown in Fig. S1, CV is also used to characterize the binding of CH19 to Trastuzumab but CV is not sensitive enough for detection. Here, non-Faradic EIS is used for characterizing Trastuzumab binding with CH19/CS7 SAM for its detection. Figure S2 shows the Nyquist plot of CH-19 peptide sensor before (black) and after (red) Trastuzumab addition (final concentration 20 µg/mL) using 2mm diameter electrodes. Significant impedance change is observed after Trastuzumab addition. To better demonstrate the impedance change induced by Trastuzumab addition, $\Delta Z_{mod} = Z^c_{mod} - Z^0_{mod}$, the absolute change (Δ) of impedance magnitude (Z_{mod}) before and after Trastuzumab addition and $\%\Delta Z_{mod} = \frac{\Delta Z_{mod}}{Z^0_{mod}}$, relative impedance change induced by Trastuzumab addition are plotted vs. frequency in Figure S2a and S2b, respectively. Z^c_{mod} represents Z_{mod} at concentration c (lowercase, to differentiate symbol capitalized C for capacitance). As shown in Figure S2b, ΔZ_{mod} at frequency above 1Hz equals to zero, this is because the high frequency impedance represents solution resistance, which is negligibly changed after Trastuzumab addition. Meanwhile, the proposed sensor is a capacitive sensor, addition of Trastuzumab mainly changes the capacitance of the system, that is, ΔZ_{mod} at low frequency range. Thus the impedance change ΔZ_{mod} at low frequency (0.1-1 Hz) is used for characterizing peptide-Trastuzumab binding. $\%\Delta Z_{mod}$ vs. frequency (0.1-1 Hz) is plotted in Figure S2c. In Figure S2c, at low frequency, $\%\Delta Z_{mod}$ increases as frequency decreases. 9% maximum impedance change is obtained at 0.1 Hz. Note, in this report, 0.1Hz is the minimum frequency as impedance at frequency <0.1 Hz, would take a long time (tens of minutes). Due to consideration of sensor response time, frequency below 0.1Hz was not studied. However, since the signal change is small, maximum 9% impedance change at 0.1Hz due to binding reactions as discussed previously, signal amplification is necessary. Thus we develop an exceptional simple and straightforward dilution strategy for amplifying non-Faradic signal as discussed below.

As discussed earlier, the differential capacitance consists of double layer capacitance C_{dl} and sensing layer capacitance C_{sl} as described in equation 3. Upon binding with Trastuzumab, C_{dl} and C_{sl} will change accordingly. As discussed previously, since the double layer capacitance C_{dl} is much larger than the sensing layer capacitance C_{sl}, thus the differential capacitance is dominated by sensing layer capacitance C_{sl}. Contribution from double layer capacitance C_{dl} change is negligible. Correspondingly, the detected signal is mainly determined by the sensing layer capacitance change upon binding with Trastuzumab. Via dilution, the double layer capacitance C_{dl} decreases due to increased diffuse layer thickness (equation 2) while dilution effect on C_{sl} is negligible. By tuning the double layer capacitance C_{dl} to be small via buffer dilution, it exhibits significant change upon Trastuzumab binding to contribute to the total differential capacitance change. The dilution method has been proven to successfully enhance signal as shown in Figure 1a, in which

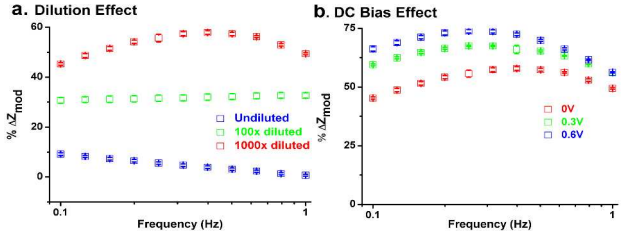

Figure 1. (a) Dilution effect on signal amplification ($\%\Delta Z_{mod}$): undiluted PBS (blue), 100x (green) and 1000x (red) diluted PBS. (b) DC bias effect on signal amplification ($\%\Delta Z_{mod}$): 0V (red), 0.3V (green) and 0.6V (blue) (vs. Ag/AgCl QRE, AC: 5 mV). Data are based on 2mm CH19/CS7 mixed peptide sensor with addition of 20 µg/mL Trastuzumab.

$\%\Delta Z_{mod}$ in undiluted PBS (blue), 100x (green) and 1000x (red) diluted PBS are compared to demonstrate the significant amplification strategy using dilution method. Corresponding ΔZ_{mod} upon dilution is plotted in Figure S3a. Figure 1a and S3a showed that 1000x diluted PBS gave the largest signal for both $\%\Delta Z_{mod}$ and ΔZ_{mod}. Figure S3a showed that ΔZ_{mod} was frequency dependent and increased as frequency decrease. In undiluted PBS, a maximum ΔZ_{mod} of 0.1 MΩ was obtained. Upon 100x dilution, ΔZ_{mod} increased to 0.3 MΩ upon Trastuzumab binding. When PBS solution was further diluted 1000x, ΔZ_{mod} increased to 0.6 MΩ. Figure 1a showed the 1000x diluted PBS resulted in the largest signal change $\%\Delta Z_{mod}$ ~50% compared to <10% in undiluted PBS and 30% in 100x diluted PBS. The above results clearly demonstrate the successful signal amplification strategy using dilution method. 1000x diluted PBS is used in later experiments as it gives the largest signal change.

2.1 DC bias effect on the CH19 peptide capacitance sensor

Since the double layer capacitance C_{dl} is also potential dependent, peptide sensor performance at different DC bias is studied here for optimization. Preliminary data are plotted as $\%\Delta Z_{mod}$ (relative impedance change) and ΔZ_{mod} (absolute impedance change) for comprehensive demonstration of impedance change. Relative impedance change $\%\Delta Z_{mod}$ in 1000x diluted PBS at various DC bias (0V, 0.3V and 0.6V) are shown in Fig 1b, while corresponding absolute impedance change ΔZ_{mod} upon dilution is plotted in Figure S3b. Figure S3b shows that at 0V, a maximum absolute impedance change ΔZmod of 0.6 MΩ at 0.1 Hz is obtained. As the DC bias increased to 0.3V, the maximum ΔZ_{mod} at 0.1 Hz increases to 0.8 MΩ. But further increase of the DC bias to 0.6V decreases the maximum ΔZ_{mod} at 0.1 Hz back to 0.6 MΩ which overlaps with the data obtained at 0V. For relative impedance change $\%\Delta Z_{mod}$, Figure 1b clearly demonstrated that $\%\Delta Z_{mod}$ increases from ~50% at 0V to ~62% (0.3V) and ~70% (0.6V). At 0V DC bias, the maximum $\%\Delta Z_{mod}$ is obtained at 0.4 Hz, and this frequency shifts to +0.2-0.3Hz when 0.6 V DC bias is applied. While for ΔZ_{mod}, the maximum ΔZ_{mod} is achieved at 0.1 Hz. In consideration of a larger signal for both ΔZ_{mod} and $\%\Delta Z_{mod}$, 0.2 Hz is selected for later experiment. Meanwhile, 0V is selected for later experiment instead of 0.6V which gives the largest $\%\Delta Z_{mod}$ since the applied bias DC potential could affect the peptide SAM layer, which is discussed in another report.[35] Meanwhile zero volt requires little input energy which is beneficial for the future low power point of care sensor device. Since the temperature and environmental change can change the open circuit potential which subsequently affects the interface peptide SAM properties, open circuit potential is not used, as this will cause a significant drift of impedance. In conclusion, later impedance experiments are performed using the optimized parameters: 0V DC bias (since other DC bias potentials affect peptide SAM and the open circuit potential is also not selected due to environment and temperature alteration can cause impedance change), 0.2 Hz frequency (for optimization of both $\%\Delta Z_{mod}$ and ΔZ_{mod}) in 1000x diluted PBS.

2.2 Single Frequency EIS for real-time monitoring of Trastuzumab

The impedance spectra analysis is important to study the solution ionic strength, DC bias, and measurement frequency effects on the sensor analytical performance. But it is not the method of choice for the biosensor since the complete frequency scan take tens of minutes and is not suitable for real-time monitoring. Here, single frequency impedance method at the optimized DC bias (0V) and frequency (0.2Hz) in 1000x diluted PBS saline solution is tested for real-time monitoring of Trastuzumab concentrations. We use a microelectrode with a 25 μm diameter to demonstrate higher spatiotemporal resolution and sensor miniaturization potential. Figure 2a shows the SEM image of the 25 μm (diameter) electrode footprint. After mechanical cleaning, the microelectrode is electrochemically cleaned in 0.05M H_2SO_4, as shown in Figure S4a. Cyclic voltammetry in 1mM 1:1 $K_3Fe(CN)_6$:$K_4Fe(CN)_6$ before and after surface modification is used to confirm the successful immobilization of peptides. As shown in Figure S4b, after immobilization with CH19 and CS7 peptides, the redox peak at ~0.2V disappears. This is due to the blocked accessibility of redox molecule to the electrode surface that results from the immobilized peptide SAM barrier.

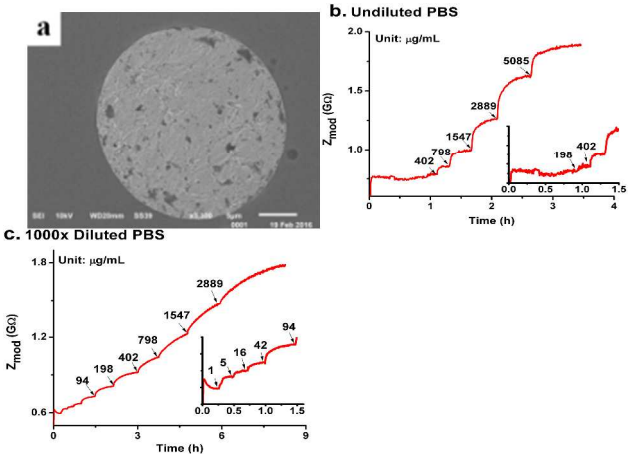

Figure 2. (a) SEM images of a 25 μm gold electrode. Single frequency EIS of 25 μm CH19 peptide sensor with various Trastuzumab concentrations in undiluted (b) and 1000x diluted (c) PBS. Impedance change at low concentration is shown in inset: undiluted PBS 0-402 μg/mL and 1000x diluted PBS 0-94 μg/mL.

For the impedance technique, impedance drifting over time has remained an issue. This is due to the change of the open circuit potential resulting from the environmental condition change such as temperature. The peptide biointerface structure at solution interface is dynamic which can also lead to baseline signal change. We incorporate a pre-conditioning method to overcome the impedance drifting issue of the biointerface. A constant 0V DC bias is applied until stable impedance is obtained (Figure S5 with details of the method), and then Trastuzumab titration is initiated. Figure 2b showed the

single frequency EIS real-time monitoring of the peptide sensor in an undiluted PBS. The impedance change upon Trastuzumab addition was shown, with inset indicated the change at low concentration. In undiluted PBS, a concentration of ~200 μg/mL is required to induce a noticeable impedance change (The reported concentration is the final concentration in PBS solution after Trastuzumab addition). The corresponding titration calibration curve was plotted in Figure 3 (blue symbol) for comparison with data obtained in 1000x diluted PBS. A linear range 0-2889 μg/mL is obtained with limit of detection 112 μg/mL (S/N=3) and a sensitivity of 0.04192 $(\mu g/mL)^{-1}$.

Figure 2c demonstrates the enhanced sensor performance in 1000x diluted PBS. Impedance change at low concentration is shown in inset, which clearly demonstrated that in a diluted condition, a significant impedance increase is observed with only 1 μg/mL Trastuzumab. The corresponding titration calibration curve is plotted in Figure 3 (red symbol). A linear range is obtained at 0-16 μg/mL, with a limit of detection of 0.22 μg/mL (S/N=3) and a sensitivity of 0.888 $(\mu g/mL)^{-1}$. In 1000x diluted PBS the dissociation constant is Kd=531 μg/mL, while in undiluted PBS Kd=$1.06x10^4$ μg/mL. A significant binding affinity increase is obtained when the PBS saline solution is 1000x diluted. The binding affinity changed is attributed to the ionic strength effect on the structure of CH19 peptide mimotope conformation instead of the pH change. Dilution significantly changes the solution ionic strength which can impact the peptide properties and subsequently affect the binding affinity.[35] Figure 3 clearly demonstrated that upon 1000x dilution, the sensor analytical performance has been enhanced significantly. The LOD decreases 500 times from 112 μg/mL in undiluted PBS to 0.22 μg/mL in 1000x diluted PBS. The sensitivity also increases 20 times from 0.04192 $(\mu g/mL)^{-1}$ in undiluted PBS to 0.888 $(\mu g/mL)^{-1}$ in 1000x diluted PBS.

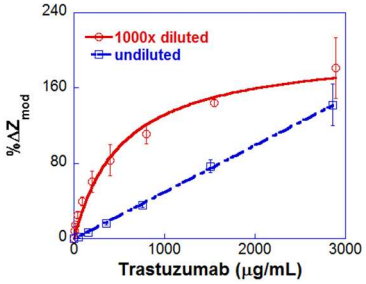

Figure 3. Signal amplification by dilution based on CH19 peptide sensor in undiluted (blue symbol) and 1000x diluted (red symbol) PBS. Solid lines represent fitting for each calibration curve. Electrode size: 25 μm.

2.3 Planar electrodes for biosensor response time optimization

In order to reduce the sensor response time that takes minutes to 1h as shown in Figures 2b and 2c, a 2 mm (diameter) planar electrode has been designed for Trastuzumab detection. The planar electrode has been integrated into a home-made cell for Trastuzumab quantification at stirring condition (see Figure S6 for electrode design). The real-time impedance change over time and corresponding titration curve is shown in Figure 4. As shown in Figure 4a, the significant improvement of using a planar electrode is that the response time is reduced to less than 1 minute, which is probably due to faster mass transport results from the different electrochemical sensor set-up in which we used a home-made Kel-F cell (the planar electrodes were mounted) that requires a smaller amount of PBS (1.2ml compared to 4ml for 25 μm sensor) and the relative larger electrode area. Meanwhile, a linear range is obtained at 0-1.98 μg/mL with a slightly increased sensitivity of 1.22 $(\mu g/mL)^{-1}$ and a comparable LOD of 0.21 μg/mL compared to 25 μm sensor is achieved. A systematic investigation of the parameters that contributed to the sensor performance improvement is ongoing.

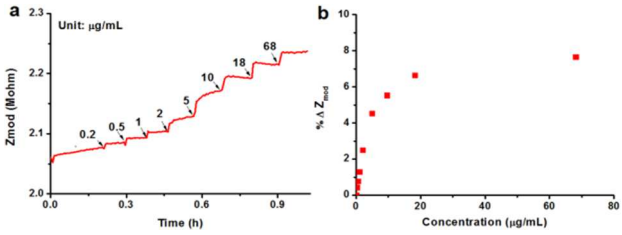

Figure 4. Single frequency EIS of planar CH19 peptide sensor for Trastuzumab quantification in 1000x diluted PBS: (a) real-time impedance monitoring; (b) Trastuzumab titration calibration curve (0-68 μg/mL). Electrode size: 2mm

3. Sensor Characterization

In this section, a full investigation of the biosensor reliability has been performed. Peptide biosensor selectivity, resistance to biofouling and reusability have been characterized.

3.1 Selectivity

The selectivity characterization was shown in Figure 5. A series of antibody cancer drugs: Bevacizumab (Avastin), Ofatumumab (Arzerra), Obinutuzumab (Gazyva), Panitumumab (Vectibix), and Rituximab (Rituxan) were used as negative control. Figure 5 clearly demonstrates sensor selectivity for Trastuzumab over other cancer drugs. The opposite response observed for ofatumumab (Arzerra) addition might indicate the sensor is capable for simultaneous multiple analytes detection.

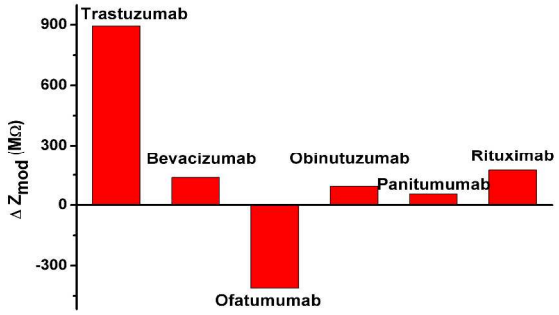

Figure 5. CH19 peptide based sensor selectivity in 1000x diluted PBS with 2.33 mg/mL drugs (final concentration in PBS). Electrode size: 25 μm

3.2 Reusability

The peptide biosensor is shown to be reusable. After tested with Trastuzumab, the sensing surface is regenerated by soaking in 4M guanidine thiocyanate for 1h. The original and regenerated sensing surfaces have been characterized using cyclic voltammetry in 1mM 1:1 (v/v) $K_3Fe(CN)_6$: $K_4Fe(CN)_6$ solution, which shows no obvious difference (Figure 6a).[36] But the single frequency EIS confirms that the impedance increases after regeneration,[35] this probably indicates a more ordered and compact SAM structure is formed after regeneration. The Trastuzumab titration calibration curves for the original and regenerated sensor are compared in Figure 6b, which almost overlapped. This confirms the reusability of the proposed sensor.

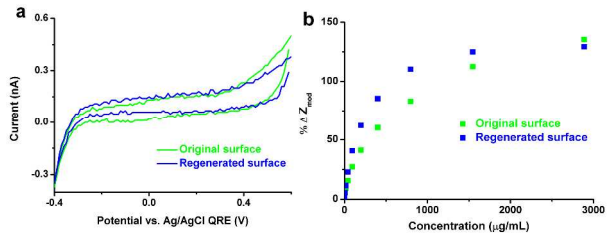

Figure 6. (a) CV of original (green) and regenerated (blue) 25μm CH-19 sensor in 1mM 1:1 (v/v) $K_3Fe(CN)_6$: $K_4Fe(CN)_6$ solution. (b) Titration curve of original (green) and regenerated (blue) CH19 sensor for Trastuzumab quantification in 1000x diluted PBS at 0.2Hz. Electrode size: 25μm.

3.3 Resistance to Biofouling

Biofouling, which is normally encountered in a serum environment detection, was also tested here in order to investigate the application of the proposed sensor using the clinical samples. As shown in Figure S7a, after a stable impedance is obtained, 4 μL undiluted serum is added into 1000x diluted PBS. Due to the serum addition, Z_{mod} increased. Impedance is allowed to stabilize after serum addition, and then the Trastuzumab titration is initiated in the presence of serum. The impedance change at low concentration was shown as inset. In the presence of serum, noise level increased (5MΩ before serum addition and 10MΩ after serum addition) while the signal change was reduced due to the biofouling effect (as shown in Figure 2C, without serum, addition of 1 μg/ml Trastuzumab increased impedance significantly while Figure S7a showed that in the presence of serum, ~94 μg/ml Trastuzumab was required for a significant impedance change). Therefore the signal to noise ratio was reduced, for example, with 94 μg/ml Trastuzumab, S/N was 43 when serum was absent, while S/N decreased to 10 in the presence of serum. This resulted in a decreased limit of detection of 16 μg/ml in the presence of serum. The corresponding titration calibration curve was shown in Figure S7b, which demonstrated successful Trastuzumab quantification even under biofouling effect introduced by undiluted serum addition.

CONCLUSION

In this work, we demonstrated a reagent free and label free peptide based biosensor using non-faradic impedance readout. This is the first report of Trastuzumab detection using electrochemical method based on non-Faradaic impedance. As the signal amplification is achieved through optimization of double layer capacitance of a peptide SAM biointerface upon dilution, the proposed method is general for non-Faradaic sensing. We overcome the drawback of the low sensitivity non-faradic impedance sensing with a new signal amplification strategy using a dilution method and peptide SAM biointerface. The smallest size of peptide mimotope (MW=1-3 kDa), allows a high density of them to be surface- immobilized and the compact and dense peptide sensing layer reduce the background noises compared to the large antibody and proteins. By using diluted PBS buffer, it allows for increased sensitivity for detecting and measuring disease biomarkers (i.e. therapeutical antibody drug Trastuzumab). A simple and straight forward dilution method was shown to enhance sensor performance significantly: limit of detection has decreased 500 times and with 20 times increased sensitivity. We further demonstrate for real-time Trastuzumab detection using miniaturized planar microelectrode. The response time has been optimized to within minute using a planar electrode with slightly improved sensitivity. Furthermore, the peptide sensor is highly selective, functional in serum (biofouling still exist, but the reported peptide sensor is still capable of quantification in serum) and is reusable. Thus, molecular biosensors based on a peptide SAM with high probe densities and uniformity in combination with non-Faradic impedance readout is a promising platform for point of care biosensor applications.

ASSOCIATED CONTENT

Supporting Information

Additional information as noted in text and Figure S1-S7. The Supporting Information is available free of charge on the ACS Publications website.

AUTHOR INFORMATION

Corresponding Author

* E-mail: zeng@oakland.edu.

Notes

The authors declare no competing financial interest.

ACKNOWLEDGMENTS

X. Zeng acknowledges support from the Oakland University Research Excellent Funds. This project was a continuation of the early project funded under NIH 1R21EB009513-01A1. Zeng would like to thank Dr. Hongwei Qu at Oakland University for SEM imaging, Dr. Yu-Hwa Lo, Dr. Ping-Wei Chen and Wei Cai for providing planar electrodes. We like to thank Dr. Yuqin Shang's preliminary work on this study.

REFERENCES

(1) Berggren, C.; Bjarnason, B.; Johansson, G. *Electroanalysis* **2001**, *13*, 173.

(2) Mirsky, V. M.; Riepl, M.; Wolfbeis, O. S. *Biosensors & Bioelectronics* **1997**, *12*, 977.
(3) Yu, X. B.; Lv, R.; Ma, Z. Q.; Liu, Z. H.; Hao, Y. H.; Li, Q. Z.; Xu, D. K. *Analyst* **2006**, *131*, 745.
(4) Ma, K. S.; Zhou, H.; Zoval, J.; Madou, M. *Sensors and Actuators B-Chemical* **2006**, *114*, 58.
(5) Rickert, J.; Gopel, W.; Beck, W.; Jung, G.; Heiduschka, P. *Biosensors & Bioelectronics* **1996**, *11*, 757.
(6) Bontidean, I.; Berggren, C.; Johansson, G.; Csoregi, E.; Mattiasson, B.; Lloyd, J. A.; Jakeman, K. J.; Brown, N. L. *Analytical Chemistry* **1998**, *70*, 4162.
(7) Jayant, K.; Singhai, A.; Cao, Y. Q.; Phelps, J. B.; Lindau, M.; Holowka, D. A.; Baird, B. A.; Kan, E. C. *Sci Rep* **2015**, *5*.
(8) Lin, S. P.; Vinzons, L. U.; Kang, Y. S.; Lai, T. Y. *ACS Appl. Mater. Interfaces* **2015**, *7*, 9866.
(9) Cecchetto, J.; Fernandes, F. C. B.; Lopes, R.; Bueno, P. R. *Biosensors and Bioelectronics* **2017**, *87*, 949.
(10) Ebrahimi, A.; Dak, P.; Salm, E.; Dash, S.; Garimella, S. V.; Bashir, R.; Alam, M. A. *Lab Chip* **2013**, *13*, 4248.
(11) Kazemi, S. H.; Shanehsaz, M.; Ghaernmaghami, M. *Mater. Sci. Eng. C-Mater. Biol. Appl.* **2015**, *52*, 151.
(12) Shang, Y. Q.; Singh, P. R.; Chisti, M. M.; Mernaugh, R.; Zeng, X. Q. *Analytical Chemistry* **2011**, *83*, 8928.
(13) Maple, L.; Lathrop, R.; Bozich, S.; Harman, W.; Tacey, R.; Kelley, M.; Danilkovitch-Miagkova, A. *J. Immunol. Methods* **2004**, *295*, 169.
(14) Jamieson, D.; Cresti, N.; Verrill, M. W.; Boddy, A. V. *J. Immunol. Methods* **2009**, *345*, 106.
(15) Damen, C. W. N.; de Groot, E. R.; Heij, M.; Boss, D. S.; Schellens, J. H. M.; Rosing, H.; Beijnen, J. H.; Aarden, L. A. *Anal. Biochem.* **2009**, *391*, 114.
(16) Zhang, B.; Galusha, J.; Shiozawa, P. G.; Wang, G. L.; Bergren, A. J.; Jones, R. M.; White, R. J.; Ervin, E. N.; Cauley, C. C.; White, H. S. *Analytical Chemistry* **2007**, *79*, 4778.
(17) Liu, J.; Kvetny, M.; Feng, J. Y.; Wang, D. C.; Wu, B. H.; Brown, W.; Wang, G. L. *Langmuir* **2012**, *28*, 1588.
(18) Liu, J.; Wang, D. C.; Kvetny, M.; Brown, W.; Li, Y.; Wang, G. L. *Analytical Chemistry* **2012**, *84*, 6926.
(19) Liu, J.; Wang, D. C.; Kvetny, M.; Brown, W.; Li, Y.; Wang, G. L. *Langmuir* **2013**, *29*, 8743.
(20) Helmhotz, H. L. F. v. *Ann. Physik* **1879**, *7*, 337.
(21) Grahame, D. C. *Chemical reviews* **1947**, *41*, 441.
(22) Gouy, G. *J. Phys. Radium* **1910**, *9*, 457.
(23) Gouy, G. *Compt. Rend.* **1910**, *149*, 654.
(24) Chapman, D. L. *Phil. Mag.* **1913**, *25*, 475.
(25) Bard, A. J.; Faulkner, L. R. *Electrochemical Methods: Fundamentals and Applications*; 2nd ed.; Wiley: New York, 2000.
(26) Stern, O. *Z Elektrochem.* **1924**, *30*, 508.
(27) Goes, M. S.; Rahman, H.; Ryall, J.; Davis, J. J.; Bueno, P. R. *Langmuir* **2012**, *28*, 9689.
(28) Ianeselli, L.; Grenci, G.; Callegari, C.; Tormen, M.; Casalis, L. *Biosensors & Bioelectronics* **2014**, *55*, 1.
(29) Katz, E.; Willner, I. *Electroanalysis* **2003**, *15*, 913.
(30) Kurzatkowska, K.; Ostatna, V.; Hamley, I. W.; Doneux, T.; Palecek, E. *Electrochimica Acta* **2013**, *106*, 43.
(31) Berggren, C.; Johansson, G. *Analytical Chemistry* **1997**, *69*, 3651.
(32) Miura, Y.; Kimura, S.; Kobayashi, S.; Imanishi, Y.; Umemura, J. *Biopolymers* **2000**, *55*, 391.
(33) Park, J. Y.; Park, S. M. *Sensors* **2009**, *9*, 9513.
(34) Moreno-Hagelsieb, L.; Lobert, P. E.; Pampin, R.; Bourgeois, D.; Remacle, J.; Flandre, D. *Sensors and Actuators B-Chemical* **2004**, *98*, 269.
(35) Leo, N.; Liu, J.; Archbold, I.; Tang, Y.; Zeng, X. *Langmuir* **2017**, *in press*.
(36) Shan, Y. Ph.D. Dissertation, Oakland University, Rochester, MI, 2013.